

Second-order effects of magnetic hyperfine interaction on NMR spectra in the $M_2CuX_4 \cdot 2H_2O$ compounds. II. Fine structure due to indirect coupling of nuclear spins

W. J. Looyestijn, T. O. Klaassen, and N. J. Poulis
Kamerlingh Onnes Laboratorium, Leiden, The Netherlands
 (Received 1 December 1978)

The indirect coupling of nuclear spins via the hyperfine interaction with the electron-spin system has been known for years. It is often discussed as an important source of line broadening in saturated (anti) ferromagnets. The experiments presented in this paper mainly concern such an interaction between only two nuclear spins. Due to the weak exchange interaction, in combination with the fact that the ligands are bonded pairwise to the magnetic ion, a well-resolved fine structure on ligand NMR lines has been observed. A theoretical description is given that explains completely the observed field and temperature dependences of the line shapes, as well as the isotope effects. Also a second fine-structure mechanism has been observed which originates from the influence of the copper nuclear spin on the local electron-spin magnetization.

I. INTRODUCTION

In Paper I,¹ it has been mentioned that several years ago a complicated fine structure had been found in the NMR spectra of some ligand nuclei in $Rb_2CuCl_4 \cdot 2H_2O$ and isomorphous compounds.^{2,3} At that time no suitable explanation for the observed fine structure could be given although several mechanisms were investigated. A new, more careful study of these fine structures was started and presently attention was also given to the spectrum of the less abundant ^{37}Cl isotopes. In this paper we prove that these fine structures originate from two basically different mechanisms. The first one is an indirect interaction between two identical (ligand) nuclear spins, involving the components of their hyperfine interaction perpendicular to the external field. This indirect interaction is closely related to the familiar Suhl-Nakamura interaction^{4,5} which is known to be the origin of NMR line broadening in several (anti)ferromagnets. However, owing to the actual ligand coordination in the $M_2CuX_4 \cdot 2H_2O$ compounds in high field a well-resolved fine structure is observed, which then yields the unique opportunity to study this indirect interaction in all details and compare it with theory.

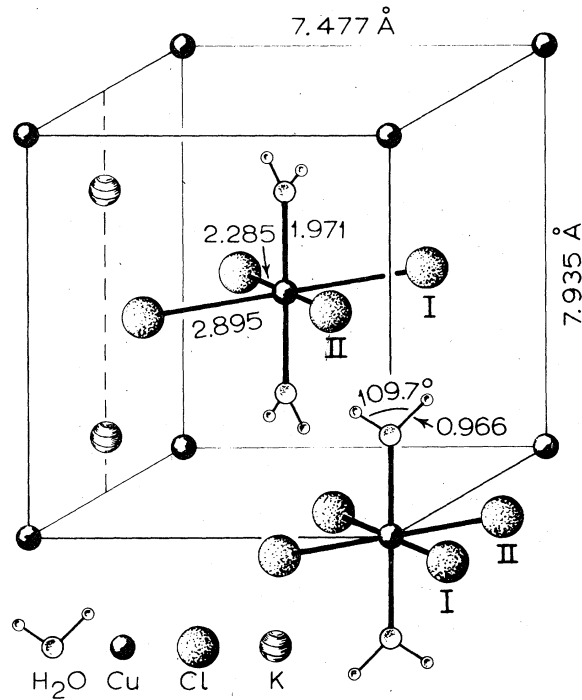
The competing second mechanism is also an indirect one, but now between nuclear spins at different crystallographic sites. This second interaction arises through the influence of the copper nuclear spin upon the (local) expectation value $\langle S \rangle$ of the unpaired electron spin via its large hyperfine interaction. The ligand nuclear spins probe in this way the orientation of the copper nuclear spin. This copper-ligand interaction involves the components of the

respective hyperfine interactions parallel to the external field. One can observe it best in low field.

Although in certain cases the effects of both interactions are observed simultaneously, the measured fine structure can now be unraveled completely. To avoid complex discussions both mechanisms will be described separately. The experimental data presented here have been selected in order to illustrate both effects separately.

II. CRYSTALLOGRAPHIC AND MAGNETIC STRUCTURE OF THE $M_2CuX_4 \cdot 2H_2O$ COMPOUNDS

Crystals with the $M_2CuX_4 \cdot 2H_2O$ structure have tetragonal symmetry with space group $P4_2/mnm$. In Fig. 1 the unit cell of $K_2CuCl_4 \cdot 2H_2O$ is shown. The copper ion at (0,0,0) has a six coordination (D_{2h} symmetry). The distorted octahedral surrounding consists of two strongly bonded $Cl_{(II)}$ ions at $\pm(0.21, 0.21, 0)$, two weakly bonded $Cl_{(I)}$ ions at $\pm(0.27, -0.27, 0)$, and two water molecules with the oxygen ions at $\pm(0, 0, 0.25)$. The protons at $\pm(0.07, 0.07, \pm 0.31)$ form hydrogen bridges with the $Cl_{(I)}$ ions belonging to the nearest-neighbor copper octahedra. The two members of each of these three pairs of ligands are fully identical, except that they can be different isotopes, e.g., ^{35}Cl and ^{37}Cl . The nearest-neighbor copper ions at $(\pm\frac{1}{2}, \pm\frac{1}{2}, \pm\frac{1}{2})$ are related to the copper ion at (0,0,0) by a 4_2 axis parallel to the c axis. Consequently, nuclei belonging to nearest-neighbor octahedra are in general magnetically nonequivalent. Even when the external field is applied along the c axis, only the parallel components

FIG. 1. Crystal structure of $K_2CuCl_4 \cdot 2H_2O$.

of the interaction tensors are equivalent; the perpendicular components however are interchanged.

The magnetic properties of these compounds are described satisfactorily by the three-dimensional bcc Heisenberg model for ferromagnets. Curie temperatures are of the order of 1 K.²

In order to avoid line broadening by an inhomogeneous distribution of demagnetizing fields over the sample, these were polished into spheres of about 6-mm diameter.

The experiments mentioned here have been performed in a 4He bath. The sample holder has been mounted in a cardan suspension, by which the sample can be oriented perfectly from outside the cryostat. The NMR signals have been obtained with a set of marginal oscillators. Frequency sweep, field modulation, and second-harmonic lock-in detection have always been used for the actual measurements.

III. INDIRECT COUPLING OF NUCLEAR SPINS

A. Theory

For the derivation of the explicit expression for the indirect coupling of nuclear spins we use the same approach as we did in Paper I for the pseudoquadrupolar interaction. Consider a system containing one electron spin $S = \frac{1}{2}$, to which two nuclear spins I and J are coupled by their respective hyper-

fine interactions \vec{A}^I and \vec{A}^J . Again, the total Hamiltonian is divided into two parts. The first contains, apart from the Zeeman interactions and the nuclear quadrupolar interactions, the components of the hyperfine interaction parallel to the external field. The second term due to the transverse components of \vec{A}^I and \vec{A}^J ,

$$\begin{aligned} \mathcal{H}' = & \frac{1}{4}(A_{xx}^I + A_{yy}^I)(I_+S_- + I_-S_+) \\ & + \frac{1}{4}(A_{xx}^I - A_{yy}^I)(I_+S_+ + I_-S_-) \\ & + \frac{1}{4}(A_{xx}^J + A_{yy}^J)(J_+S_- + J_-S_+) \\ & + \frac{1}{4}(A_{xx}^J - A_{yy}^J)(J_+S_+ + J_-S_-) \end{aligned} \quad (1)$$

is regarded as a perturbation to the first term. Again, as in Paper I, in second order an energy shift of the unperturbed ground state arises, which can be interpreted as due to an effective interaction Hamiltonian of the nuclear spins I and J . This Hamiltonian contains (of course) the pseudoquadrupolar terms $\mathcal{H}_I^{\text{eff}}$ and $\mathcal{H}_J^{\text{eff}}$, which have been discussed in Paper I.

Apart from these terms, cross terms in I and J appear in the effective Hamiltonian which are proportional to $\langle m_I m_J | I_\alpha I_\beta | m_I m_J \rangle$ with $\alpha, \beta = \pm$. These latter terms can be regarded as matrix elements of an effective two-spin Hamiltonian, describing an indirect interaction between two spins I and J , i.e.,

$$\begin{aligned} \mathcal{H}_{IJ}^{\text{eff}} = & 2\Delta[(A_{xx}^I A_{xx}^J + A_{yy}^I A_{yy}^J)(I_+J_- + I_-J_+) \\ & + (A_{xx}^I A_{xx}^J - A_{yy}^I A_{yy}^J)(I_+J_+ + I_-J_-)] \end{aligned} \quad (2)$$

again with $\Delta = (16g_{zz}\mu_B H)^{-1}$. It should be recalled here that the indices x , y , and z refer to a frame of reference in which z is fixed in the direction of the external field. Moreover, it is assumed that the external field is applied along a principal axis of both \vec{A}^I and \vec{A}^J . General orientations can be treated in a similar way, but the expression for $\mathcal{H}_{IJ}^{\text{eff}}$ becomes rather complicated and less transparent.

In magnetic materials, the electron spins are coupled by their exchange interaction. As in Paper I, the total magnetic system is now described using a spin-wave or excitation model. The influence of this exchange coupling on $\mathcal{H}_{IJ}^{\text{eff}}$ proves to be twofold. First, the field dependence of the magnitude of the effective interaction is changed (as for the pseudoquadrupolar interaction). Second, now an interaction also arises between nuclei coupled to different electron spins. The effective Hamiltonian $\mathcal{H}_{IJ}^{\text{eff}}$ keeps the same form as Eq. (2), but Δ is replaced by

$$\Delta(\vec{r}) = \sum_{\vec{k}} 2S e^{i\vec{k} \cdot \vec{r}} / 16N \omega_{\vec{k}} \quad (3)$$

Here \vec{r} is the vector connecting the electron spins to which I and J are coupled. When I and J are coupled to the same electron spin, $\vec{r} = 0$. In Fig. 2 the field dependence of $h\Delta(\vec{r})$ is shown for different values

of \bar{r} , calculated for a bcc lattice. The coordinates of \bar{r} are expressed in units of the lattice constants. The curves for $\bar{r} = (\frac{1}{2}, \frac{1}{2}, \frac{1}{2})$ etc. have been omitted for reasons to be discussed later on. Figure 2 shows that for $r > 0$ $\Delta(\bar{r})$ is always at least an order of magnitude less than $\Delta(0)$, and decreases faster with increasing field than $\Delta(0)$ does.

In Paper I it was shown that the pseudoquadrupolar interaction has the same form as an electric quadrupolar interaction and can thus be treated in the usual way. The influence of the indirect interaction $\mathcal{J}_{ij}^{\text{eff}}$ on the I and J spectra is somewhat more complicated and proves to depend strongly on whether I and J are magnetically identical or not. When I and J are unlike spins, for instance spins of different isotopes or spins of nuclei at different magnetic sites, the effect of $\mathcal{J}_{ij}^{\text{eff}}$ on the spectra can be calculated, treating $\mathcal{J}_{ij}^{\text{eff}}$ as a perturbation on the usual nuclear-spin Hamiltonians $\mathcal{H}_I^{(0)}$ and $\mathcal{H}_J^{(0)}$. Following standard techniques it can easily be seen that in second order a shift of the unperturbed energies $E_{m_I}^{(0)}$ and $E_{m_J}^{(0)}$ arises which is of the order of

$$(4\Delta A_{ii}^I A_{ii}^J)^2 / (E_{m_I}^{(0)} - E_{m_J}^{(0)}) \quad (4)$$

The experimental conditions are usually such that this shift is negligibly small (e.g., in the hereafter described experiments on the chlorine nuclei this shift is at the most 100 Hz).

However, for like spins, i.e., spins of the same isotope, at magnetically identical sites and with the same quadrupolar interaction, the influence of $\mathcal{J}_{ij}^{\text{eff}}$ cannot be calculated by a perturbation method, because the energy levels if I and J now coincide, and hence the perturbation series is not convergent. Therefore, the total Hamiltonian of spins I and J , including $\mathcal{J}_{ij}^{\text{eff}}$, has

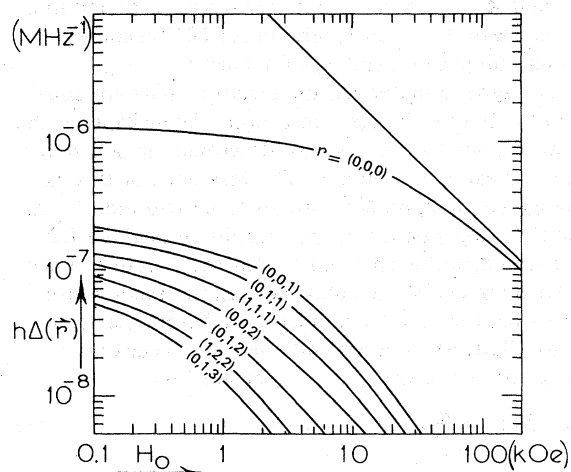


FIG. 2. Calculated field dependence of $h\Delta(\bar{r})$ for $T_c = 1$ K. The straight line represents $h\Delta = (16g\mu_B H)^{-1}$.

to be diagonalized to obtain the exact energy levels. In this situation the shift will be of the order of $4\Delta A_{ii}^I A_{ii}^J$, which can be larger than the line width. Consequently, when observing a transition of I , a fine structure can be expected due to the different orientation possibilities for J . The detailed shape of the fine structure depends strongly on the actual total nuclear-spin Hamiltonian. In a semiclassical picture this means that, because the spins I and J have equal precessing frequencies, the coupling between their transverse components does not average zero. This is analogous to the familiar $\frac{3}{2}$ effect in the proton-proton dipolar interaction.⁶ In the discussion of the experimental data the results of these calculations are presented.

B. Experimental results and discussion

1. Fine structure

In this section we will prove that the observed fine structure in the $\text{Cl}_{(\text{II})}$ NMR lines of the $\text{M}_2\text{CuX}_4 \cdot 2\text{H}_2\text{O}$ compounds can be understood completely when the above-derived indirect interaction between like spins is incorporated in the nuclear-spin Hamiltonian. Both chlorine isotopes (^{35}Cl and ^{37}Cl)

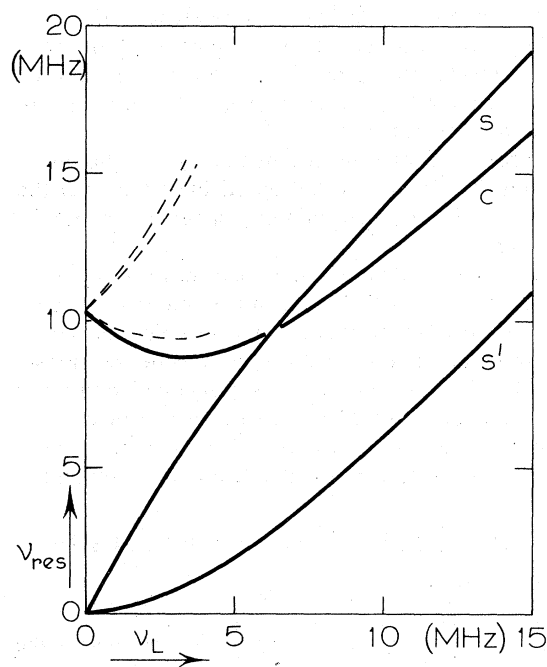


FIG. 3. Calculated NMR resonance frequencies for $^{35}\text{Cl}_{(\text{II})}$ ($\nu_Q = 10.3$ MHz, $\eta = 0.16$) as a function of the Larmor frequency ν_L . The total magnetic field is directed along the y axis of the EFG tensor.

TABLE I. Interaction parameters for (a) $\text{Rb}_2\text{CuCl}_4 \cdot 2\text{H}_2\text{O}$ and (b) $\text{Rb}_2\text{CuBr}_4 \cdot 2\text{H}_2\text{O}$. The principal axes c , γ , and γ' are along Cu-O, Cu-Cl_(I), and Cu-Cl_(II), respectively (see Refs. 2 and 3).

		$\frac{1}{2h}A_c$ (MHz)	$\frac{1}{2h}A_\gamma$ (MHz)	$\frac{1}{2h}A_{\gamma'}$ (MHz)	ν_Q (MHz)	η
(a)	$^{35}\text{Cl}_{(I)}$	0.14	0.85	0.03	2.10	0.70
	$^{35}\text{Cl}_{(II)}$	3.80	2.94	-27.31	10.30	0.16
	^{17}O	44.44	32.95	32.70	1.24	0.43
	^{63}Cu	-14.1	-228	-20.1	43.7	0.16
	^{87}Rb	-1.45	-1.15	-1.15	0.803	0
(b)	$^{79}\text{Br}_{(I)}$	1.41	5.13	1.20	12.45	0.64
	$^{79}\text{Br}_{(II)}$	8.22	6.04	126.2	81.8	0.22
	^{17}O	46.23	34.79	34.44	1.28	0.47
	^{63}Cu	-39.8	-265	-36.2	40.8	0.17
	^{87}Rb	-1.70	-1.37	-1.37	0.808	0

have nuclear spin $I = \frac{3}{2}$. The quadrupolar interaction at the Cl_(II) site is in most experimental situations comparable in magnitude with the magnetic interaction (see Table I). Therefore a general analytical expression for the Cl_(II) energy levels can not be given. A numerical diagonalization of the 16×16 matrix of the total Hamiltonian of two spins $I = \frac{3}{2}$ including $\mathcal{H}_{II}^{\text{eff}}$ has been performed, yielding the resonance frequencies and the corresponding transition probabilities. In Fig. 3 the $^{35}\text{Cl}_{(II)}$ resonance frequencies, calculated from the unperturbed Hamiltonian, are plotted as a function of the Larmor frequency $\nu_L = (\gamma/2\pi)H + (1/h)A_{zz}\langle S \rangle$. The field is applied along the y axis of the EFG tensor. In general only three transitions can be observed experimentally, which are indicated in Fig. 3 by the drawn lines. In a strong field (i.e., $\nu_L > \nu_Q$) there results the well-known spectrum consisting of a central line c and two satellite lines s and s' . Towards lower fields ($\nu_L \ll \nu_Q$) this spectrum changes drastically. Incorporation of the perturbation $\mathcal{H}_{II}^{\text{eff}}$ in the calculations has the consequence that each of these lines is split up. As this splitting is too small to be indicated on the scale of Fig. 3, in Figs. 4, 5, and 6 the calculated fine structure of each of the three lines is given. At two values of ν_L drawings of the line shapes are given in the insets of the figures, to compare with the hereafter presented experimental line shapes. For the values of the parameters in $\mathcal{H}_{II}^{\text{eff}}$ the values of the $^{35}\text{Cl}_{(II)}$ hyperfine interaction, as given in Table I, have been used. The field dependence of Δ has not been taken into account in these figures, to keep them generally applicable. To obtain Figs. 4, 5, and 6 the fixed value $h\Delta = 5 \times 10^{-7} \text{ MHz}^{-1}$ has been used.

In Fig. 7 three $^{35}\text{Cl}_{(II)}$ NMR lines are shown that are observed in a 99.7-at.% ^{35}Cl enriched sample of $\text{Rb}_2\text{CuCl}_4 \cdot 2\text{H}_2\text{O}$. A magnetic field of 20.2 kOe is applied along the crystallographic c axis (y axis of the EFG tensor). The temperature is 1.2 K and the relative magnetization is 0.95, leading to $\nu_L = 10 \text{ MHz}$ for $^{35}\text{Cl}_{(II)}$. The theoretical fine structures also given in this figure have been derived from the calculated fine structures at $\nu_L = 10 \text{ MHz}$ (Figs. 4, 5, and 6) using the appropriate value of $\Delta(0)$ at $H = 20.2 \text{ kOe}$ (Fig. 2). No fit on the horizontal scale has been made; the fine structures of all these three lines have been calculated straightforwardly using only known values of hyperfine interactions, exchange constant,

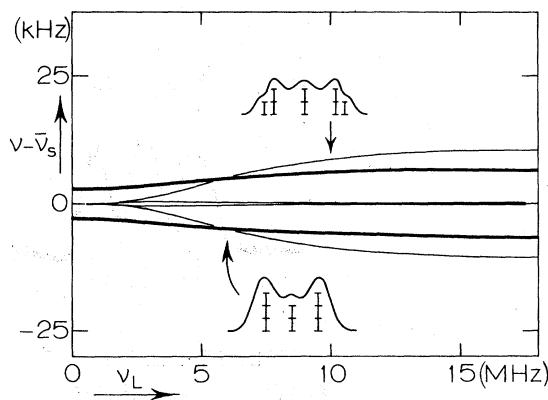


FIG. 4. Calculated fine structure of the satellite line s of Fig. 3 due to H_{II}^{eff} using a fixed value $\Delta = 5 \times 10^{-7} \text{ MHz}^{-1}$ and $A_{xx} = A_\gamma$ and $A_{yy} = A_{\gamma'}$ for $^{35}\text{Cl}_{(II)}$ (see Table I).

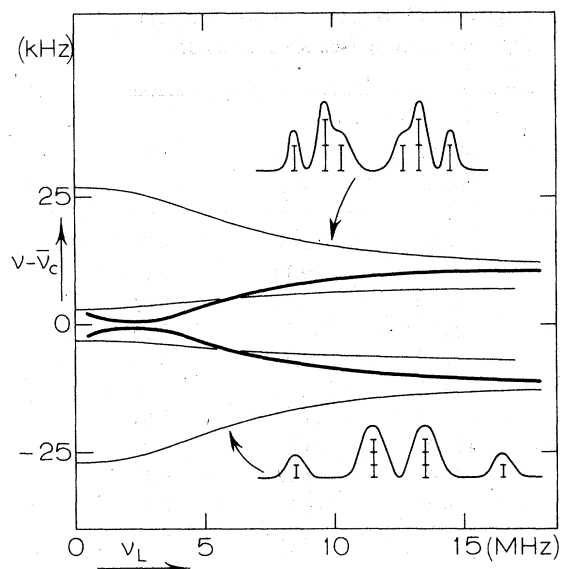


FIG. 5. Calculated fine structure of the central line c of Fig. 3.

and applied field. The agreement between these calculations and experiments is excellent. This fine structure thus arises from the indirect interaction between the two $^{35}\text{Cl}_{(\text{II})}$ nuclear spins belonging to the same copper octahedron. In Fig. 8(c) the central $^{35}\text{Cl}_{(\text{II})}$ line is shown for the same sample, but now at $H = 10$ kOe ($\nu_L = 6$ MHz). It can be seen that the relative positions of the different fine-structure lines have been changed compared to the situation at 20 kOe (Fig. 7), in accordance with the calculations shown in the inset in Fig. 5 for $\nu_L = 6$ MHz. Because of the increase of $\Delta(0)$ towards lower field the overall splitting is larger.

It has been shown above that the effect of $\mathcal{J}C_{ij}^{\text{ff}}$ is

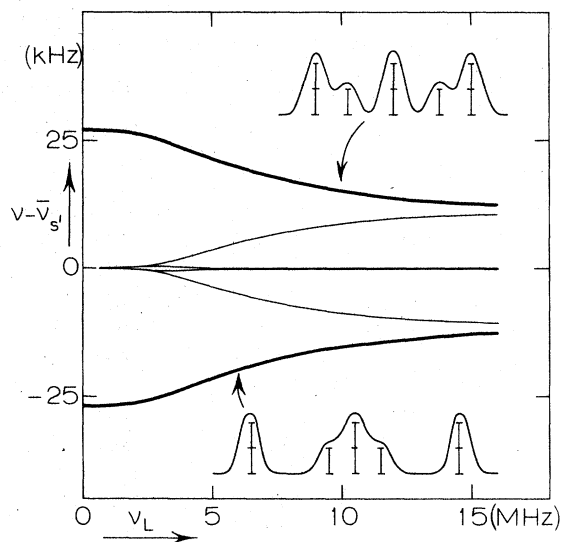


FIG. 6. Calculated fine structure of the satellite line s' of Fig. 3.

completely different for like spins and unlike spins. This conclusion is illustrated in Fig. 8. Again in Fig. 8(a) the central $^{35}\text{Cl}_{(\text{II})}$ resonance line is shown under the same conditions as in Fig. 8(c), but now in an isotopically nonenriched crystal. The natural abundances of the chlorine isotopes are 75-at.% ^{35}Cl and 25-at.% ^{37}Cl . In this sample a quarter of the ^{35}Cl nuclei has a ^{37}Cl neighbor. For this 25% of the ^{35}Cl nuclei the effect of $\mathcal{J}C_{ij}^{\text{ff}}$ is negligible, resulting in an extra, unsplit line in the center of the resonance pattern in Fig. 8(a). The corresponding $^{37}\text{Cl}_{(\text{II})}$ line in the same crystal is shown in Fig. 8(b). Only a quarter of the ^{37}Cl nuclei can interact with a like nucleus, and hence three quarters of the total ^{37}Cl line intensity remains unsplit. In this figure the four ^{37}Cl

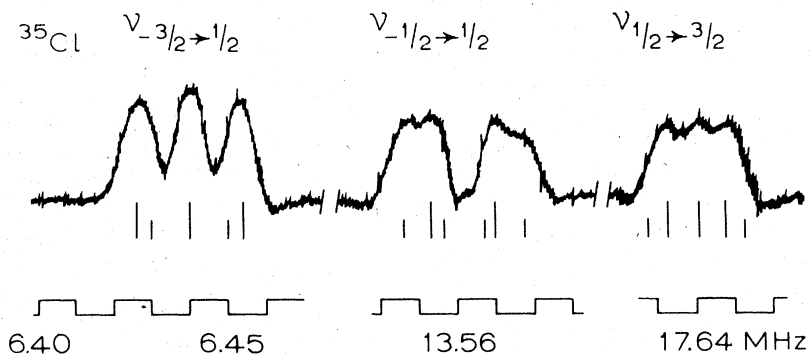


FIG. 7. Experimental $^{35}\text{Cl}_{(\text{II})}$ NMR spectrum (second derivative) at $T = 1.2$ K and $H = 20$ kOe directed along the c axis in a $\text{Rb}_2\text{CuCl}_4 \cdot 2\text{H}_2\text{O}$ sample with 99.7-at.% ^{35}Cl . The theoretical fine structure has been calculated straightforwardly.

fine-structure lines can also be seen although with the expected lesser intensity. The observed ratio of the splittings in the ^{35}Cl and ^{37}Cl spectra equals $[A(^{35}\text{Cl})/A(^{37}\text{Cl})]^2$. These results are in full agreement with the derived expression for the indirect interaction $\mathcal{H}_{ff}^{\text{eff}}$. In the isomorphous compounds¹ in which Rb has been replaced by K, NH_4 , or Cs the same fine structure is found in the $\text{Cl}_{(\text{II})}$ lines. Also in the $\text{Br}_{(\text{II})}$ lines of the two bromine compounds a fine structure has been detected. In Fig. 8(d) a $^{79}\text{Br}_{(\text{II})}$ resonance line is shown as observed in $\text{Rb}_2\text{CuBr}_4 \cdot 2\text{H}_2\text{O}$. As the abundances of ^{79}Br and ^{81}Br are equal, the shape of the resonance lines are similar for both isotopes. Again, the observed ratio of the splittings is $[A(^{79}\text{Br})/A(^{81}\text{Br})]^2$. The line shape, as shown in Fig. 8(d), can be understood completely if one takes into account the abundance of isotopes, the appropriate values of the hyperfine interactions, and the strength of the external field compared to the exchange interaction.

2. Line broadening

Between like spins belonging to different copper octahedra, an indirect interaction also exists. The

magnitude of this interoctahedron interaction is much smaller than the intraoctahedron interaction because of the \bar{r} dependence of $\Delta(\bar{r})$. The smallest \bar{r} value that has to be considered is that between next-nearest copper neighbors. Nearest-neighbor copper octahedrons, e.g., at $(0,0,0)$ and $(\frac{1}{2}, \frac{1}{2}, \frac{1}{2})$, are magnetically nonequivalent and therefore never contain like nuclear spins. Only with the field along the c axis are they equivalent, but then the term $A_{xx}^I A_{xx}^J + A_{yy}^I A_{yy}^J$ in $\mathcal{H}_{ff}^{\text{eff}}$ (2) equals $2A_x A_y$ which is much less than $A_x^2 + A_y^2$ for next-nearest neighbors, because $A_x \gg A_y$, see Table I. In a bcc lattice there are six next-nearest (second) neighbors, 12 fourth neighbors, etc. Consequently, the interoctahedron indirect interaction involves a large number of almost equally strong interacting nuclei. A multiple line splitting arises with much smaller overall splittings than that due to the intraoctahedron interaction because $\Delta(\bar{r}) \ll \Delta(0)$ for $\bar{r} > 0$. Therefore, this interoctahedron interaction results only in a line broadening of each of the fine-structure lines. In high fields the ratio $\Delta(\bar{r})/\Delta(0)$ is rather small for any $\bar{r} > 0$, so that this line broadening is rather small and the fine-structure lines can be seen well separated. With decreasing field, $\Delta(\bar{r})/\Delta(0)$ becomes larger because

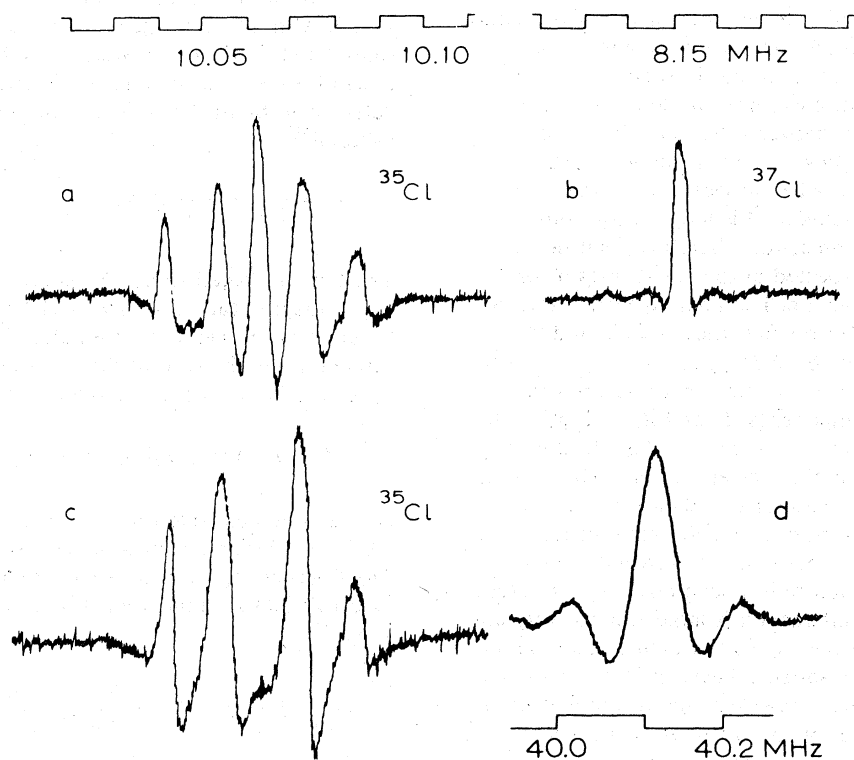


FIG. 8. Central NMR lines at $T = 1.2$ K and $H = 10$ kOe directed along the c axis. (a) and (b) in a $\text{Rb}_2\text{CuCl}_4 \cdot 2\text{H}_2\text{O}$ sample with 75-at.% ^{35}Cl and 25-at.% ^{37}Cl . (c) in a $\text{Rb}_2\text{CuCl}_4 \cdot 2\text{H}_2\text{O}$ sample with 99.7-at.% ^{35}Cl . (d) in a $\text{Rb}_2\text{CuBr}_4 \cdot 2\text{H}_2\text{O}$ sample with 50-at.% ^{79}Br and 50-at.% ^{81}Br .

$\Delta(\bar{\nu})$ increases faster than $\Delta(0)$. Consequently, the line broadening will increase faster than the line splitting. For $H \leq 8$ kOe, this broadening of the fine-structure lines has been observed experimentally. For $H \leq 5$ kOe $\Delta(\bar{\nu})/\Delta(0)$ is so large that only one broad resonance line remains, in which the fine structure has disappeared.

In the ferromagnetic state, at $T = 0.3$ K in zero external field the $\text{Cl}_{(II)}$ transitions of both chlorine isotopes have been detected having a line width of about 50 kHz, without fine structure.² The situation in the ferromagnetic state is similar to that in a weak field in the paramagnetic state in which also only a broadened line is observed, because the anisotropy field in these compounds is small.

3. Effect of $\mathcal{J}C_{ff}^{\text{ff}}$ on other NMR spectra

Now we will discuss the effect of the indirect interaction for the other nuclei in these compounds. It has been shown that a well-resolved fine structure can be expected only when this interaction occurs between the spins of two identical nuclei, of the same isotope, coupled to the same electron spin. The copper and alkali nuclei are not in such a situation, thus no fine structure can be expected in their spectra. The separation between the individual fine-structure lines exceeds only their line width (due to dipolar interactions) when at least one of the transverse components of \bar{A} is large. Inspecting Table I, it can be concluded, therefore, that no fine structure can be expected in the NMR lines of $\text{Br}_{(I)}$ and $\text{Cl}_{(II)}$ which have a rather small hyperfine interaction. Even in the resonance lines of $\text{Cl}_{(II)}$ and $\text{Br}_{(II)}$ no fine structure is observed when the magnetic field is applied along the γ' direction, because then the two relatively small components A_γ and A_c determine the strength of the indirect interaction. The third pair of ligands is formed by the oxygen nuclei of the two water molecules. The natural abundance of the only oxygen isotope that possesses a nonzero nuclear spin ^{17}O , is very small. Only in a ^{17}O enriched sample (40%) the fine structure has been observed. Because the ^{17}O hyperfine interaction is large and not very anisotropic (Table I) the ^{17}O fine structure could be observed on all five resonance lines, for any orientation of the external field. However, due to the high spin ($I = \frac{5}{2}$) the number of fine-structure lines is large. Moreover, a large number of them disappears under the unsplit line which has 60% of the total absorption intensity. Therefore no attempt has been made to give a quantitative analysis of the ^{17}O fine structure.

IV. COPPER-LIGAND INTERACTION

The foregoing part of this paper was devoted to the fine structure arising from the indirect interaction between the transverse components (I_\pm) of like spins. As already mentioned in the Introduction, the analysis of this fine structure was hindered by the fact that simultaneously a second fine structure occurs. This second interaction proves to be due to the influence of the copper nuclear spin on the local magnetization of the electron spin, and hence on the ligand internal field. This copper-ligand interaction is thus nonzero only when the magnetization is nonsaturated. However, when the magnetization is small, a large number of spin waves is present and interactions between spin waves must be taken into account. Then, a description of the magnetic system based upon a simple spin-wave model is no longer justified. Hereafter a description based on the molecular-field model will be given that provides a qualitative, as well as a quantitative explanation, of the observed copper-ligand interaction.

A. Theory

To start with, the simple model of one electron spin S , without exchange coupling, and two nuclear spins I and J , will be considered. When the fluctuations of \bar{S} are fast, the Larmor frequency of spin I is determined by the field H and the time-averaged value of \bar{S}

$$\nu_L^I = \frac{\gamma_I}{2\pi} H + \frac{1}{h} A_z^I \langle S \rangle \quad (5)$$

The time-averaged value $\langle S \rangle$ is related to the reduced magnetization m by $m = (1/S) \langle S \rangle$, and is a function of temperature and field. The total field H_t acting on \bar{S} is the sum of the external field H and the hyperfine fields due to the interaction with I and J

$$H_t = H + (m_I/g\mu_B) A_{zz}^I + (m_J/g\mu_B) A_{zz}^J$$

Hence, when considering a $m_I \rightarrow m_I'$ transition, there are $2J + 1$ possible values for H_t . When these hyperfine fields acting on \bar{S} are small compared to the external field H , expression (5) can be expanded in a series,

$$\nu_L^I = \frac{\gamma_I}{2\pi} H + A_{zz}^I \left\{ \langle S \rangle_H + \frac{\partial \langle S \rangle_H}{\partial H} \frac{m_J}{g\mu_B} A_{zz}^J + \dots \right\} \quad (6)$$

Neglecting higher-order terms, a $(2J + 1)$ -fold equidistant fine structure is expected for the resonance lines of I .

To extend this description to a ferromagnet the (super) exchange coupling between the electron spins must be taken into account. In a molecular-field model the magnetization of spin S_i is described by the implicit solution of the Curie-Weiss equations,

$$\langle S_i \rangle = S_i \tanh(x_i) \quad (7)$$

$$x_i = \frac{g\mu_B(H + \delta H)}{kT} + \frac{2zJ^{\text{ex}}\frac{1}{S}\langle S \rangle}{kT} \quad (8)$$

Here $\delta H = m_J A_{zz}^J / g\mu_B$ is the hyperfine field from the nuclear spin J_i on the electron spin S_i . Because the nuclear-spin polarization is negligible the bulk magnetization $(1/S)\langle S \rangle$ in Eq. (8) does not depend on hyperfine fields. When $|\delta H| \ll H$, formula (7) can be expanded in a Taylor series

$$\begin{aligned} \frac{1}{S_i} \langle S_i \rangle &= \frac{1}{S} \langle S \rangle + \frac{\partial \left(\frac{1}{S_i} \langle S_i \rangle \right)}{\partial x_i} \frac{g\mu_B \delta H}{kT} + \dots \\ &\approx m + m_J A_{zz}^J (1 - m^2/kT) \end{aligned} \quad (9)$$

Again, from Eqs. (5) and (9), a $(2J+1)$ -fold equidistant fine structure is expected in the NMR lines of I . The difference in Larmor frequency between the outer-fine-structure lines is given by

$$\Delta\nu_L^J = 2JS A_{zz}^J A_{zz}^I / h (1 - m^2/kT) \quad (10)$$

Generally this line splitting is not observed in NMR spectra because $\Delta\nu_L^J$ is smaller than the width of the observed resonance line. Only in peculiar situations, like those described below, can this mechanism lead to an observable fine structure.

B. Experimental results and discussion

In the series of $M_2\text{Cu}X_4 \cdot 2\text{H}_2\text{O}$ the Cu hyperfine interaction has a very large component A_γ (Table I). It can thus be expected that the splitting in Eq. (10) will be large only when the field is directed along the γ direction. Experimentally under this condition the discussed fourfold splitting ($I^{\text{Cu}} = \frac{3}{2}$) has been observed on all resonance lines of ^{17}O , $^{35}\text{Cl}_{(\text{II})}$, and $^{37}\text{Cl}_{(\text{II})}$. This splitting arises for both chlorine isotopes in a similar way, in contrast with the forementioned Cl-Cl indirect interaction. The Cu-Cl effect could be studied best on the $^{37}\text{Cl}_{(\text{II})}$ lines, because especially the $^{37}\text{Cl}_{(\text{II})}$ lines hardly exhibit the Cl-Cl fine structure. The $^{35}\text{Cl}_{(\text{II})}$ lines on the contrary exhibit a very complicated fine structure, because of the simultaneous effect of both the Cl-Cl interaction and the Cu-Cl interaction. Both interactions can be studied separately. For instance, the Cu-Cl fine structure on the $^{35}\text{Cl}_{(\text{II})}$ lines vanishes for $\vec{H} \parallel \vec{c}$ because A_c^{Cu} is small, whereas the Cl-Cl is hardly observed on the $^{37}\text{Cl}_{(\text{II})}$ lines.

In Fig. 9 a typical $^{37}\text{Cl}_{(\text{II})}$ line shape, demonstrating the Cu-Cl four fold fine structure, is shown. In Fig. 10 the observed $\Delta\nu_L$ has been plotted against $(1 - m^2)/T$, in order to compare these experiments with expression (10). On the vertical scale $\Delta\nu_L^J / (1/h) A_{zz}^J S$ has been plotted to obtain the same scale for all ligand nuclei. The magnetization used on the horizontal scale has been derived experimentally. The ^{17}O and ^{37}Cl data in this figure are collected from experiments in a large field and temperature region, $1 \text{ kOe} < H < 10 \text{ kOe}$ and $1.2 \text{ K} < T < 4 \text{ K}$. In this region the same value for $(1 - m^2)/T$ can be obtained in several ways, which results always in the

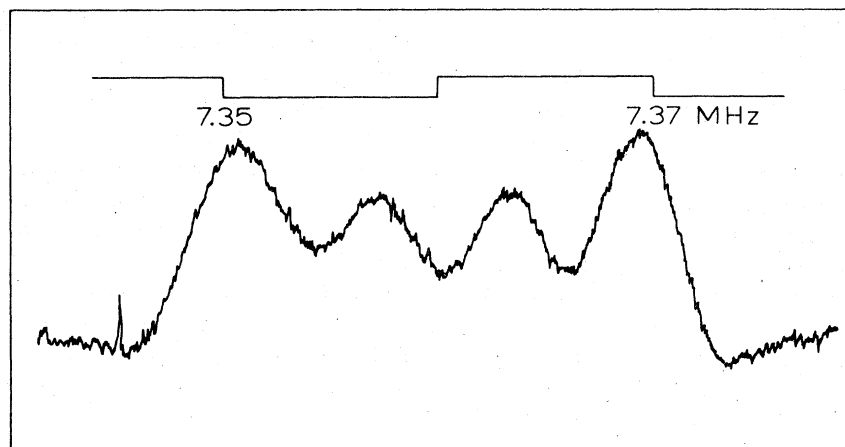


FIG. 9. Shape of the central $^{37}\text{Cl}_{(\text{II})}$ NMR line (second derivative) in $\text{Rb}_2\text{CuCl}_4 \cdot 2\text{H}_2\text{O}$ at $T = 1.2 \text{ K}$ and $H = 7.37 \text{ kOe}$ applied along the γ direction, showing the fourfold copper-ligand fine structure.

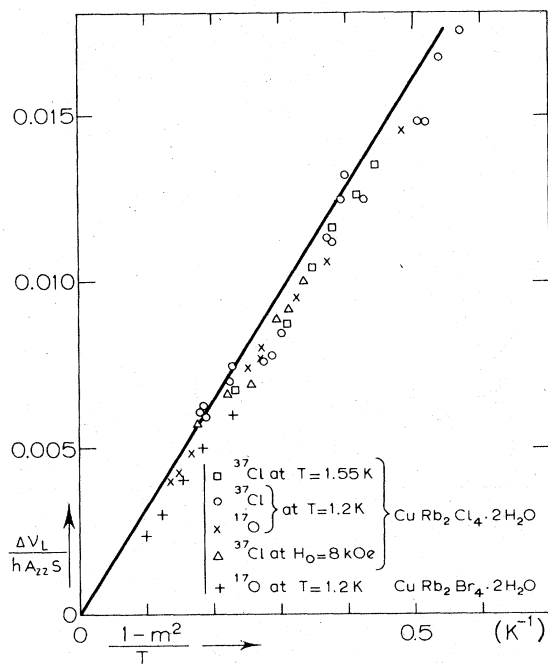


FIG. 10. Comparison of the experimental results of the copper-ligand interaction with the molecular-field prediction (straight line).

same value for $\Delta\nu_L$. In weak fields the fourfold structure can not always be observed properly. When the width of each of the four lines exceeds the distance between the four lines, on the second derivative, only a two fold splitting is observed. In Fig. 11 such a line is shown together with a fit of a set of four Gaussian lines at equal distance. A fit with Lorentzian lines appears to be impossible. In Sec. III B it was shown that in weak field the line width of the individual lines is mainly due to the indirect interaction with many other nuclear spins. This gives approximately a random broadening and thus a Gaussian-like line shape has to be expected. This Gaussian line shape is also in agreement with earlier calculations and measurements of the line shape of NMR lines broadened by a Shul-Nakamura interaction.⁷

In the bromine compounds the copper-ligand interaction has been observed only in the ^{17}O lines (see Fig. 10). In the $\text{Br}_{(\text{II})}$ lines the Cu-Br splitting could not be observed, because the line width due to the

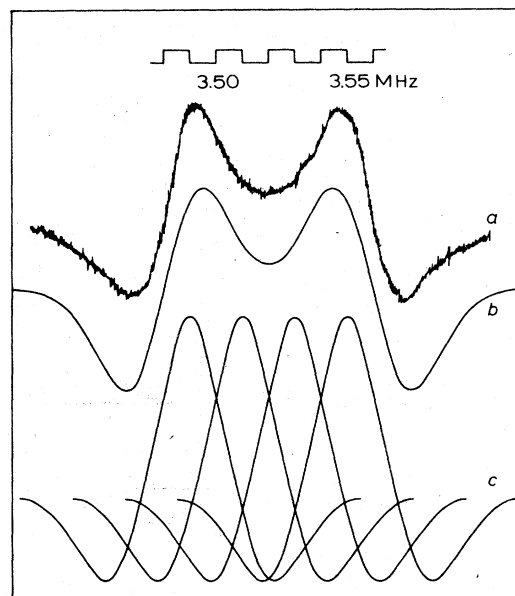


FIG. 11. Shape of the central $^{37}\text{Cl}_{(\text{II})}$ NMR line (a) (second derivative) in $\text{Rb}_2\text{CuCl}_4 \cdot 2\text{H}_2\text{O}$ at $T=1.2\text{ K}$ and $H=1.60\text{ kOe}$ applied along the γ direction. The calculated line shape (b) is a composition of four identical Gaussian lines (c).

indirect Br-Br interaction is relatively too large to make the Cu-Br interaction observable. From the values for the hyperfine interactions listed in Table I it can be calculated that also for the Rb, $\text{Cl}_{(\text{I})}$, and $\text{Br}_{(\text{I})}$ nuclei this line splitting is smaller than the line width and thus is not observable.

The straight line in Fig. 10 represents the molecular-field prediction [Eq. (10)], calculated straightforwardly. The agreement with the experimental data is very good. It can thus be concluded that in a wide region of temperature and magnetic field the variations of the local magnetization can be described satisfactory with a simple molecular-field model.

ACKNOWLEDGMENT

This work is part of the research program of the "Stichting voor Fundamenteel Onderzoek der Materie (FOM)", which is financially supported by the "Stichting voor Zuiver Wetenschappelijk Onderzoek (ZWO)".

¹W. J. Looyestijn, T. O. Klassen, and N. J. Paulis, Phys. Rev. B **19**, 4363 (1979) (preceding paper).

²T. O. Klassen, W. J. Looyestijn, and N. J. Paulis, Physica (Utrecht) **77**, 43 (1974) (Commun. Kamerlingh Onnes Lab. 411 a).

³W. J. Looyestijn, T. O. Klassen, and N. J. Paulis, Physica (Utrecht) B **93**, 349 (1978) (Commun. Kamerlingh Onnes

Lab. 434 a).

⁴H. Suhl, Phys. Rev. **109**, 606 (1958).

⁵T. Nakamura, Progr. Theor. Phys. **20**, 542 (1958).

⁶G. E. Pake, J. Chem. Phys. **16**, 327 (1948).

⁷E. A. Turov and M. P. Petrov, *Nuclear Magnetic Resonance in Ferro- and Antiferromagnets*. (Halsted, New York, 1972), Vol. V.